2017 IEEE/RSJ International Conference on Intelligent Robots and Systems (IROS)
September 24–28, 2017, Vancouver, BC, Canada

Collision Selective LGMDs Neuron Models Research Benefits from a Vision-based Autonomous Micro Robot

Qinbing Fu, Cheng Hu, Tian Liu and Shigang Yue

Abstract— **The developments of robotics inform research across a broad range of disciplines. In this paper, we will study and compare two collision selective neuron models via a vision-based autonomous micro robot. In the locusts' visual brain, two Lobula Giant Movement Detectors (LGMDs), i.e. LGMD1 and LGMD2, have been identified as looming sensitive neurons responding to rapidly expanding objects, yet with different collision selectivity. Both neurons have been modeled and successfully applied in robotic vision system for perceiving potential collisions in an efficient and reliable manner. In this research, we conduct binocular neuronal models, for the first time combining the functionalities of LGMD1 and LGMD2 neurons, in the visual modality of a ground mobile robot. The results of systematic on-line experiments demonstrated three contributions of this research: (1) The arena tests involving multiple robots verified the effectiveness and robustness of a reactive motion control strategy via integrating a bilateral pair of LGMD1 and LGMD2 models for collision detection in dynamic scenarios. (2) We pinpointed the different collision selectivity between LGMD1 and LGMD2 neuron models, which fulfill corresponding biological research. (3) The utilized micro robot may also benefit researches on other embedded vision systems as well as swarm robotics.**

I. INTRODUCTION

For an autonomous robot, the ability of perceiving imminent collision, in a timely and robust manner, is essential. However, it is still a pronounced challenge for safe navigations of robots without human interventions, especially mixed with dynamic objects. There are now many collision-detecting sensors like the infra-red, laser, radar, ultrasound, vision, or combination of these sensors. However, those sensing modalities are restricted heavily to the applications of small robots, due to their size, reliability and/or energy consumption. For robotic applications, the neuromorphic vision sensors [1], in comparison with traditional sensing modalities using the segmentation and registration based computer vision techniques [2], can cope with the degree of complexity in real physical world for collision detection more efficiently that fulfill the utility in small mobile robots.

As the result of hundreds of millions of years evolution, the biological visual systems have provided abundant source of inspirations for modeling artificial vision systems for collision detection. Especially the insects' visual neural networks could be ideal models to design collision free visual systems, which have demonstrated amazing ability of interacting with the dynamic world yet with very limited number of neurons relative to the vertebrates' visual systems.

In locusts, a group of Lobula Giant Movement Detectors (LGMDs) have been discovered by biologists for decades, and two of them, i.e. LGMD1 and LGMD2, have been identified as looming sensitive neurons responding rigorously to approaching objects with high frequency spikes, amongst other kinds of visual challenges [3]–[6]. Although both neurons share the same colliding cues that reacting to the expanding edges of an object, the different collision selectivity between LGMD1 and LGMD2 have been revealed [3], [5], [6]. More specifically, since compared to LGMD1, LGMD2 matures earlier in juvenile locusts living on the ground [5], its collision selectivity is tuned to only darker objects approaching embedded in bright background, i.e a light-to-dark luminance change [3]; while LGMD1 is sensitive to both illuminating and darkening caused by brighter and darker objects looming [3].

Many computational models have been conducted for LGMD1, e.g. [7]–[9], but very few for LGMD2 [10], [11]. Since LGMDs models have low computational-cost yet high efficiency, they have been applied in robots for help navigation mixed with obstacles [10], [12]–[15]. In addition, two related researches also have assessed their distinctive characteristics, suggesting LGMD2 possesses enhanced collision selectivity for ground vision-based robots [10], [11]. However, LGMD2 has the defect of not responding to light objects looming against dark backgrounds. Due to their specific advantages and shortcomings for collision recognition, we expected to inspect the collaborative performance in collision-detecting tasks, via combining their functionalities.

In this study, we set up a binocular vision system by integrating LGMD1 and LGMD2 neuron models into the visual modality of a mobile micro-robot. Compared to previous arena tests [10], [15] that only a single robot was applied and mixed with multiple obstacles, we examined its performance in an arena involving multiple autonomous robots with on-board binocular neuron models. In addition, a directional motion control method with a bilateral pair of LGMD1 and LGMD2 neuronal models was applied for reactive collision avoidance behaviors in the arena tests.

In the following sections, the LGMDs neuronal models with algorithms and parameters setting will be presented in Section II. The utilized autonomous micro robot and the systematic on-line experiments with results and analysis will be illustrated in Section III. Finally, we give a conclusion in Section IV.

This work was supported by the grants of EU FP7 projects LIVCODE(295151), HAZCEPT(318907) and EU Horizon 2020 project STEP2DYNA(691154). We thank Dr. Tomáš Krajník and Mr. Peter Lightbody for helping build the robots localization systems in the arena tests.

All authors are with the Computational Intelligence Lab (CIL), School of Computer Science, University of Lincoln, Lincoln, UK, LN6 7TS. First and Corresponding author: Qinbing Fu, Email: qifu@lincoln.ac.uk

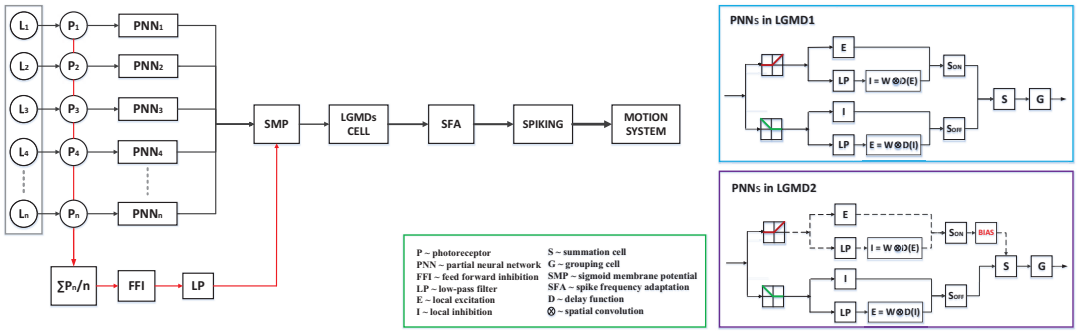

Fig. 1. The schematic illustration of a general LGMDs neuron model with ON and OFF pathways: the notations of neural network components are shown in the green box. The inputs are gray-scale luminance (L) in a matrix form. For each local pixel, the visual processing in the partial neural network (PNN) of LGMD1 model (in the blue box) differs from that of LGMD2 model (in the purple box) - a 'bias' is put forth in each ON-channel of LGMD2 model. Both neuron models share a same FFI pathway depicted by red arrows. The outputs are spikes towards further motion system.

II. THE EMBEDDED VISION SYSTEM

In this section, we will present the embedded vision system and the motion control strategy adopted in the arena tests. With respect to the biological research milestones in not only the looming sensitive neurons in locusts [3]–[6], [16], but also the direction selective neurons in flies and vertebrates [17], we propose a general model (Fig. 1) for conducting both LGMD1 and LGMD2 neurons, with separated ON/OFF pathways processing visual information in parallel: brightness increments and decrements flow into ON and OFF channels by onset and offset responses respectively. Each polarity pathway is constituted by a cascade of sub-layers with spatiotemporal lateral connections. Such a bio-plausible structure is vital to achieve their different looming selectivity. Essentially, a latest modeling work with ON and OFF pathways conducted the direction selective visual neurons for extracting translating motion cues [18]. In comparison with that, the proposed LGMDs neural networks possess different methodologies for visual processing in the dual-pathways detecting objects moving in depth rather than in four cardinal directions. In addition, we construct a biophysical mechanism - spike frequency adaptation [19], shaping its selectivity to approaching over receding and translation movements. A spiking code is also applied for potential collision recognition in robotic applications.

It is also worth emphasizing here, compared to other traditional vision systems for collision detection, the proposed neuron models only involve low-level image processing methodologies, detects potential collision by responding to the expanding edges of an object. Those computationally expensive algorithms, like target classification, scene analysis and machine learning methods are not applied at all.

A. The LGMDs Neuronal Models

LGMD1 and LGMD2 neuron models share a general signal processing pipeline illustrated in Fig. 1. However, the partial neural networks (PNNs) in LGMD1 differ from those in LGMD2, i.e. a bias is put forth in all ON channels of LGMD2 models rigorously sieving onset responses for achieving its specific looming selectivity to darker objects - a preference to the light-to-dark luminance change.

1) Photoreceptors: The first layer of the visual neural network consists of photoreceptors arranged in a 2D matrix form. The number of them is decided by the amount of pixels (n) within the retina (P_1 to P_n in Fig. 1). Each photoreceptor retrieves corresponding gray-scale luminance (L) and obtains the 'motion' information by the luminance change at each local pixel between successive frames:

$$P_{x,y}(t) = L_{x,y}(t) - L_{x,y}(t-1) \tag{1}$$

2) Partial Neural Networks: The pre-synaptic area to LGMD was postulated to be reconciled by the ON and OFF polarity cells as early in 1970s [16]. As depicted in PNNs, the luminance changes are fed into the 'half-wave' rectifiers leading to onset and offset responses for parallel ON and OFF channels, represented by:

$$\begin{aligned} P^{ON}_{x,y}(t) &= (P_{x,y}(t) + |P_{x,y}(t)|)/2, \\ P^{OFF}_{x,y}(t) &= |(P_{x,y}(t) - |P_{x,y}(t)|)|/2 \end{aligned} \tag{2}$$

After that, the signals relayed by ON and OFF cells are processed with spatiotemporal lateral connections within each pathway. First, in the ON pathway, ON cells elicit onset responses by brightness increments, i.e. the excitation is conveyed directly to its counterpart cell in the next layer, whilst the inhibition is delayed relative to the excitation, formed by convolving surrounding delayed-excitations:

$$\begin{aligned} E^{ON}_{x,y}(t) &= P^{ON}_{x,y}(t), \\ I^{ON}_{x,y}(t) &= \sum_{i=-r}^{r} \sum_{j=-r}^{r} D^{ON}_{x+i,y+j}(t) \cdot W(i,j) \end{aligned} \tag{3}$$

where r denotes the size of inhibited area. W indicates the convolution matrix. Compared to previous state-of-the-art LGMDs neuron models, e.g [7], [10], that the delayed information only spreads out to their neighboring cells rather than to their direct counterparts, we allow the self-inhibition mechanism, which has been proposed recently [6]. In addition, $D^{ON}_{x,y}$ is the low-pass filtered excitation with τ_1 denoting a time constant in millisecond:

$$\frac{dD^{ON}_{x,y}(t)}{dt} = \frac{1}{\tau_1}(E^{ON}_{x,y}(t) - D^{ON}_{x,y}(t)) \tag{4}$$

Similarity for the visual processing in the OFF pathway, OFF cells relay information to two flows for excitations and inhibitions. However, compared to signals processing in ON pathway, excitations are delayed relative to inhibitions, caused by offset responses of brightness decrements:

$$\begin{aligned} I_{x,y}^{OFF}(t) &= P_{x,y}^{OFF}(t), \\ E_{x,y}^{OFF}(t) &= \sum_{i=-r}^{r}\sum_{j=-r}^{r} D_{x+i,y+j}^{OFF}(t) \cdot W(i,j) \end{aligned} \tag{5}$$

wherein the delay function conforms to Eq. 4. Then, in either pathway, the excitations and inhibitions depict a purely linear competition in polarity summation layers. We put forward a local bias (w) for suppressing each inhibitory flow:

$$\begin{aligned} S_{x,y}^{ON}(t) &= E_{x,y}^{ON}(t) - w \cdot I_{x,y}^{ON}(t), \\ S_{x,y}^{OFF}(t) &= E_{x,y}^{OFF}(t) - w \cdot I_{x,y}^{OFF}(t) \end{aligned} \tag{6}$$

After polarity summations, there are interactions between parallel ON and OFF channels at the summation layer. We apply a supralinear computation between polarity excitations as suggested in [20]:

$$S_{x,y} = \theta_1 \cdot S_{x,y}^{ON} + \theta_2 \cdot S_{x,y}^{OFF} + \theta_3 \cdot S_{x,y}^{ON} \cdot S_{x,y}^{OFF} \tag{7}$$

where $\{\theta_1, \theta_2, \theta_3\}$ denotes the combinations of term coefficients, allow us to represent either purely-linear or non-linear relationship between ON and OFF channels. Such a computational form plays a crucial role of achieving the different collision selectivity between LGMD1 and LGMD2 neurons - an extra bias is put forth in ON pathway for LGMD2; the coefficients are balanced for LGMD1.

In the proposed neuron models, the expanded edges represented by clustered excitations are enhanced to extract colliding objects from complex backgrounds through a simplified grouping layer (G) before the pooling stage. Essentially, it is a convolution process with an equal-weighted kernel W_g:

$$G_{x,y}(t) = \sum_{i=-r}^{r}\sum_{j=-r}^{r} S_{x+i,y+j}(t) \cdot W_g(i,j) \tag{8}$$

3) LGMDs Cells: Both LGMDs cells pool all the presynaptic local excitations from the dual-pathways in a linear manner to form the membrane potential (K), which is exponentially transformed via a sigmoid function mimics the activation of artificial neurons:

$$K_t = \sum_{x=1}^{row}\sum_{y=1}^{col} G_{x,y}(t), \;\; K_t^{'} = (1 + e^{-|K_t| \cdot (n \cdot k)^{-1}})^{-1} \tag{9}$$

where row and col are the rows and columns of the G layer. $K^{'}$ indicates the sigmoid membrane potential (SMP). The coefficient k shapes the function curve. As illustrated in Fig. 1, there is another separated pathway from the photoreceptors layer - the feed forward inhibition (FFI), which can directly suppress LGMDs neurons if a large number of photoreceptors are activated simultaneously:

$$F_t = \sum_{x=1}^{row}\sum_{y=1}^{col} |P_{x,y}(t)| \cdot n^{-1}, \frac{d\bar{F}_t}{dt} = \frac{1}{\tau_2}(F_t - \bar{F}_t) \tag{10}$$

TABLE I
THE PARAMETERS SETTING OF LGMDS NEURON MODELS

Parameter: Name, Value					
Name	Value	Name	Value	Name	Value
col	55	T_{sf}	0.001	τ_1, τ_2	$5 \sim 100$
row	72	W	0.25	T_{sp}	0.66
K_{sp}	4	W_g	1/9	τ_3	$400 \sim 1000$
r	1	k	0.3	τ_i	$20 \sim 50$ Hz
w	0.5	N_{ts}	4	$\theta_1, \theta_2, \theta_3$	$0 \sim 6$
N_{sp}	6	T_{ffi}	16	n	$col \cdot row$

where $\bar{F}_t$ denotes the postponed FFI with a time constant τ_2 in millisecond to be conveyed to the LGMDs cell. Once the FFI output exceeds its threshold level T_{ffi}, the LGMD1 or LGMD2 neuron will be immediately inhibited.

4) Spike Frequency Adaptation: To further enhance the looming selectivity of LGMD1 and LGMD2 neuron models to approaching versus receding and translation movements, we conduct a biophysical mechanism of spike frequency adaptation (SFA). It is computationally modeled as a selective high-pass filter, which only allows the membrane potential with positive-derivative profile to overcome its sieving:

$$\bar{K}_t = \begin{cases} \sigma_1 \cdot (\bar{K}_{t-1} + K_t^{'} - K_{t-1}^{'}), \; if \;\; K_t^{'} - K_{t-1}^{'} \leq T_{sf} \\ \sigma_1 \cdot K_t^{'}, \quad else \end{cases} \tag{11}$$

where T_{sf} is a very small positive real number. σ_1 denotes a coefficient calculated by $\sigma_1 = \tau_3/(\tau_3 + \tau_i)$, wherein τ_3 indicates a time constant in millisecond and τ_i is the sampling frequency of visual streams.

5) Spiking Mechanism: The sieved potential is going to invoke different amounts of spikes towards the motion system, in an exponential manner. Compared to previous LGMD1 modeling works, e.g. [7], the proposed neuron models may represent higher spike frequency, since more than one spikes could be elicited at each frame:

$$S_t^{spike} = \left\lfloor e^{[K_{sp} \cdot (\bar{K}_t - T_{sp})]} \right\rfloor \tag{12}$$

Such a function returns the largest integer less than or equal to the inside real number. K_{sp} and T_{sp} denote a coefficient and the spiking threshold respectively. Finally, a potential collision recognition is decided by:

$$COL = \begin{cases} True, \quad if \quad \sum_{i=t-N_{ts}}^{t} S_i^{spike} \geq N_{sp} \\ False, \quad otherwise \end{cases} \tag{13}$$

where N_{sp} denotes the number of continuous elicited spikes and N_{ts} indicates the number of successive frames which is normally set to be less than N_{sp} in our case.

6) Vision System Parameters Setting: The parameters of the binocular neuron models are decided empirically with consideration of functionality for implementations in the micro robot, as suggested in Table I. Both neuron models

TABLE II

THE ROBOTIC MOTION BEHAVIORS IN THE ARENA TESTS

F: go forward, R/L: turn right/left, S/SSS: stop/long stop
BR/BL: go backward then turn right/left

Condition	Motion	Condition	Motion
$DIR = Right$	R	$DIR = Left$	L
$S_t^1 = S_t^2$	S	$Default$	F
$DIR = Right \ \& \ S_t^2 \geq N_{sp}$	BR	$\bar{F}_t \geq T_{ffi}$	SSS
$DIR = Left \ \& \ S_t^1 \geq N_{sp}$	BL		

share vast majority of parameters; however, the 'bias' in ON pathway of LGMD2 model is achieved by setting θ_1 to 0, whilst $\theta_1 = \theta_2 \ \& \ \theta_1 > 0$ for LGMD1. In addition, the time parameter τ_3 in calculating the coefficient σ_1 in SFA mechanism could vary within a wide range so as to adjust the adaptation rate of neural potential. No parameter training or feedback learning algorithms are currently involved in the embedded vision system.

B. The Motion Control System

In this research, we integrated a bilateral pair of LGMD1 and LGMD2 neuron models that are in competition for reactive directional motion control. Although the biologists found that LGMD1 and LGMD2 elicit different collision avoidance behaviors for locusts [5], in this study, we assume that they reproduce the escape directions in a comparable way, since the micro robot can only run on the 2D surface.

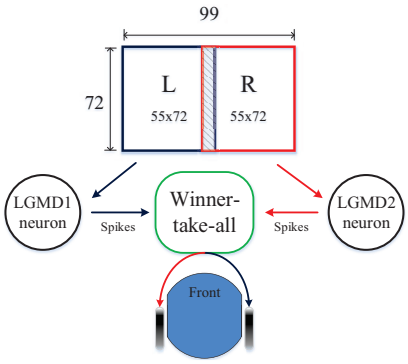

Fig. 2. The illustration of image processing in the visual modality of the micro robot and the directional motion control strategy with a bilateral pair of LGMDs neuron models: each gray-scaled frame (in full resolution of $99 \cdot 72$) is divided into two regions ($55 \cdot 72$) with a small overlapping area. By default, the left/right region of view is handled by LGMD1/LGMD2 neuron respectively. The generated spikes go through a 'winner-take-all' competition: the winner - LGMD1 or LGMD2 neuron motivates the right or left wheel to reverse for turning response of the micro robot.

More specifically, as illustrated in Fig. 2, the image view of each frame is split into two regions that handled by LGMD1 (left) and LGMD2 (right) neuron models respectively, which also correspond to the right and left wheels reversing-control for turning response. The elicited spikes are fed into a simple 'winner-take-all' strategy similar to [13], [21], for deciding

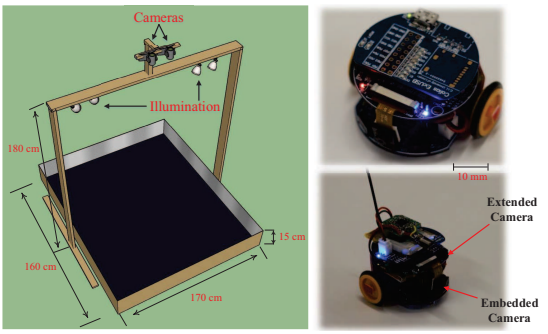

Fig. 3. The schematic diagram of the arena and micro robot in on-line tests. (1) The arena: two cameras form the top-down views for recording the overtime performances of robots and running the multi-robots localization systems. Four lights are used for illumination. The arena is with $170 \cdot 160$ cm^2 in area and the edges are with 15 cm in height. (2) The micro robot prototype: the bottom board is the motion actuator with two assembled wheels and a battery. The upper board executes the vision systems via an embedded camera; the LED lights can indicate real time events. The extension board can have varied functionality, like the bluetooth device for data transmission, and the wireless camera for the capture of frontal views.

the escape direction in avoidance behaviors:

$$DIR_t = \begin{cases} Right, \ if \ S_t^1 > S_t^2 \ \& \ \sum_{i=t-N_{ts}}^{t} S_i^1 \geq N_{sp} \\ Left, \ if \ S_t^2 > S_t^1 \ \& \ \sum_{i=t-N_{ts}}^{t} S_i^2 \geq N_{sp} \end{cases} \quad (14)$$

where S^1 and S^2 are the elicited spikes by LGMD1 and LGMD2 respectively. Occasionally, the left and right neuron models produce the same number of spikes. This would be rare for a locust, since its post-synaptic neuron to LGMD spikes at very high frequency, much higher than our modeled counterpart. However, when implemented in robots, either model works at approximately 30 Hz, its left and right LGMD models may sometimes elicit the same number of spikes at the time of escape. In addition, the FFI also affects the performance of robot, thus we initiated extra escape behaviors in the arena tests as listed fully in Table II.

III. EXPERIMENTAL EVALUATION

In this section, we will illustrate the systematic robot experiments. All the trials can be sorted into two parts: the arena tests and the angular approach tests. It is important to note that in both kinds of experiments, we set up the dark and bright environments respectively, for inspecting the performance of integrating a bilateral pair of LGMD1 and LGMD2 models. First, we will give a concise introduction to the utilized micro robot.

A. The Mobile Robot Description

In this study, the binocular LGMD1 and LGMD2 neuron models were mounted in a low-cost micro robot named 'Colias' (Fig. 3). It is used for swarm robotics [22]–[24], and bio-inspired embedded vision systems research [10], [11], [15]. It is important to state here although the Colias robot has auxiliary sensing modalities for collision detection - the

TABLE III
THE COLIAS ROBOT CONFIGURATION

Dimensions	ϕ 40 x h 32 mm
SRAM	256 Kbyte
Embedded Camera	99 x 72 YUV422 at 30 fps
Battery	320 mAh, 3.7 V
Default Linear Speed	approximately 55 mm/s
Turning Angular Speed	approximately 2π rad/s
Autonomy	$1 \sim 2$ hours

bumper infrared sensors [15], [22], [24], we only applied its embedded visual module in this research.

As illustrated in Fig. 3 and Table III, the bottom board provides power for corresponding motion behaviors as shown in Table II. The upper vision board implements the proposed neuronal models with an OV7670 camera from Omni-vision, which could reach to approximately 70 degrees of view arc. The motion and vision boards are two fundamental modules for the Colias robot. Interestingly, we can also extend it with multiple modules due to specific requirements in real time experiments, like the data communication with the hosts, the capture of first views and etc.

B. The Arena Tests

The first kind of experiment is the arena tests. The periphery of a sub-region in the arena is decorated with dark patterns densely embedding in a white background, as shown in Fig. 4d. We set up bright environment with full arena lights (Fig. 3) and the global illumination, as well as dark environment with only a single arena light for illumination respectively, for the purposes of examining the usefulness and robustness of the binocular neuron models for collision detection mixed with moving agents, as well as investigating the different looming selectivity individually.

Firstly, in the bright environment, we examine its performance of collision detection in the arena tests involving multiple (5) Colias robots running simultaneously. With the help of top-down real-time tracking systems [25], [26], we could get the very precise trajectories of each Colias robot with its specific pattern pointing out the ID. Fig. 4 illustrates a few frontal first-views recorded from the extended wireless camera of a Colias robot when it is running in the arena, representing some particular events[1], like quickly avoiding the moving robot agents (Fig. 4a, 4b), circumventing the surrounding walls (Fig. 4d), traveling towards the crossing robots (Fig. 4c). All the avoidance or waiting behaviors were invoked by the collaboration of the bilateral pair of LGMD1 and LGMD2 models, as introduced in Table II. More important, we calculate the statistical success rates for all the tested Colias robots throughout repeated arena tests. We define a successful collision detection comprises not only avoiding a potential proximity (invoked by high frequency spikes), but also waiting for a near translation movement (elicited by high level FFI output). Intuitively, Table IV

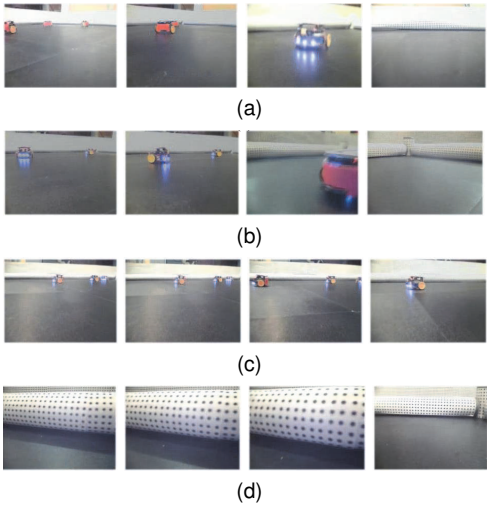

Fig. 4. Four illustrative events of the arena tests in bright environment, represented by the first views from the wireless camera of a Colias robot agent: (a) the robot-to-robot avoidance (b) two successive avoidances (c) challenged by translating robots (d) the robot-to-obstacle avoidance.

TABLE IV
THE SUCCESS RATES (SR) FOR MULTIPLE COLIAS ROBOTS

Events: Avoidance(A), Waiting(W), Colliding(C)
SR = (A + W) / (A + W + C) · 100%

ID	Avoidance	Waiting	Colliding	SR
1	769	51	21	97.50%
6	867	36	37	96.06%
10	698	80	11	98.61%
11	715	43	33	95.83%
15	743	28	51	93.80%

shows the statistics for these ID specific Colias robots running together for approximately 2 hours in total. Satisfactory results demonstrate the effectiveness and robustness of the proposed integrated and embedded LGMDs neuron models with reactive directional motion controls for Colias robots in collision-detecting tasks even against dynamic scenarios.

After that, we estimate its success rates of approaching a fixed lighter object in the dark environment simulating the situation of 'night navigation'. As well, to point out the different looming selectivity between LGMDs, we let the Colias robot approach the lighter object from left and right sides respectively[2] (Fig. 5). By default, the LGMD1 and LGMD2 models handle the left and right region of receptive field separately (Fig. 2). Fig. 5a and 5b demonstrate the Colias robot fails to recognize the colliding and hits the target approaching from the left side, yet succeeds in perceiving the collision approaching from the right side. Intriguingly, after switching the processed regions by the LGMD1 and LGMD2 models, Fig. 5c, 5d depict totally reverse reactions of the Colias robot. Moreover, the informative statistics throughout repeated tests (Table V) clearly demonstrate when challenged by lighter objects looming embedded in a dark background, the proposed binocular neuron model is not as robust as the performance in the arena tests with fully bright scenes. Even

[1]A video demo shows the first views in the supplementary attachment.

[2]The results in Fig. 5 are shown in the video attachment.

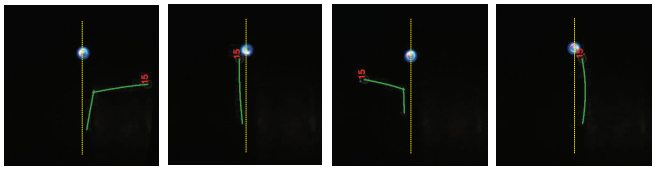

(a) (b) (c) (d)

Fig. 5. Four illustrative results of the arena tests in dark scenes - the Colias robot with the binocular neuron models implemented approaches an immobile lighter object from left and right sides. (a), (b) The left and right regions of image view are handled by LGMD1 and LGMD2 respectively. (c), (d) Conversely, the right and left regions of view are handled by LGMD1 and LGMD2 respectively. The yellow dashed line separates the two sides. The trajectory of the Colias robot with ID-15 is depicted in green line.

TABLE V

THE SUCCESS RATES FOR APPROACHING LIGHTER OBJECT

Repeat: R, Avoidance: A, SR = A / R · 100%			
Left-LGMD1 & Right-LGMD2 Approaching Side	R	A	SR
Right	50	45	90%
Left	50	10	20%
Right-LGMD1 & Left-LGMD2 Approaching Side	R	A	SR
Left	50	41	82%
Right	50	15	30%

though the LGMD1 model still performs convincingly on detecting light looming stimuli coming from its processed view region, the LGMD2 model does not - it has the defect of not responding to the dark-to-light luminance change. The experimental results perfectly match the related researches [3], [5], [6] on biological LGMD1 and LGMD2 neurons.

C. The Angular Approach Tests

The second type of experiment includes the systematic angular approach tests as illustrated in Fig. 6. We aimed to deeply investigate its collision selectivity via combining a bilateral pair of LGMD1 and LGMD2 neuron models. We collected the neural outputs of the monitoring Colias robot, containing the SMP and the spikes afterwards.

Comparative results in Fig. 7 and 8 allow the following analysis to be drawn: first, when challenged by dark angular approaching (Fig. 7), both LGMD1 and LGMD2 models represent high-level SMP and high frequency spikes, especially when challenged by direct approaching (Fig. 7c). When the dark looming stimuli come from the left side, LGMD1 model responds more vigorously and much earlier than LGMD2 (Fig. 7a, 7b). Conversely, when stimulated by the right-side angular approaches, LGMD2 contributes more significantly, spiking at higher frequency (Fig. 7d, 7e). Interestingly, when challenged against light angular approaching, Fig. 8 clearly demonstrate LGMD2 neuron is inhibited during light-looming from each angle, whilst LGMD1 is still activated - its spiking rate peaks at the direct approaching (Fig. 8c). However, it also remains quiet once the looming comes from the right side with the largest angle (Fig. 8e) like Fig. 7e.

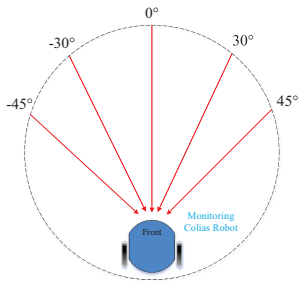

Fig. 6. The experimental illustration of the systematic angular approach tests: a motionless Colias robot at a fixed location, with the binocular neuron models implemented (left-LGMD1 and right-LGMD2), is stimulated by an approaching Colias robot from different angles repeatedly, in dark and light environments respectively. In the dark environment, the approaching robot is with the light source used in Fig. 5.

More intuitively, the statistics in Fig. 7f and 8f demonstrate the collision selectivity of the proposed binocular neuron model fully - at least one model could recognize the colliding of darker objects coming within the view arc, yet only the LGMD1 model is robust in detecting lighter objects approaching. In addition, both LGMDs neurons spike at the highest rate against the direct approaching, representing the most powerful strike from the predator to locusts.

IV. CONCLUDING REMARKS

In this research, we integrated two locust looming sensitive neuron models into the visual modality of a ground mobile robot. Although a few LGMD1 or LGMD2 based models have been successfully applied in robots, it is the first time to combine the functionality of both LGMDs neuron models to form a binocular vision system. The systematic experiments verify its efficiency and robustness with a reactive directional motion control strategy in the arena tests mixed with multiple robots. Moreover, its collision selectivity has been pinpointed fully, which well match the revealed characteristics of biological LGMD1 and LGMD2 neurons.

This study opens several directions for future research. We have shown the LGMD1 model with ON and OFF pathways is competent for utility in the dark environment for collision detection, whilst related researches have proved LGMD2 model performs more robustly compared to LGMD1 for ground robots in daylight navigation. If we could build a hybrid system with similar structures, the collision selectivity could be further enhanced. Another interesting question concerns with using the micro robot for other biological modeling researches, like the direction selective neurons.

REFERENCES

[1] G. Indiveri and R. Douglas, "Neuromorphic vision sensors," *Science*, pp. 1189–1190, 2000.

[2] G. N. DeSouza and A. C. Kak, "Vision for mobile robot navigation: a survey," *IEEE Trans. Pattern Anal. Mach. Intell.*, vol. 24, no. 2, pp. 237–267, 2002.

[3] P. J. Simmons and F. C. Rind, "Responses to object approach by a wide field visual neurone, the lgmd2 of the locust: Characterization and image cues," *J Comp Physiol A*, vol. 180, pp. 203–214, 1997.

[4] F. C. Rind and B. D. I., "Neural network based on the input organization of an identified neurone signaling impending collision," *J Neurophysiol*, vol. 75, pp. 967–985, 1996.

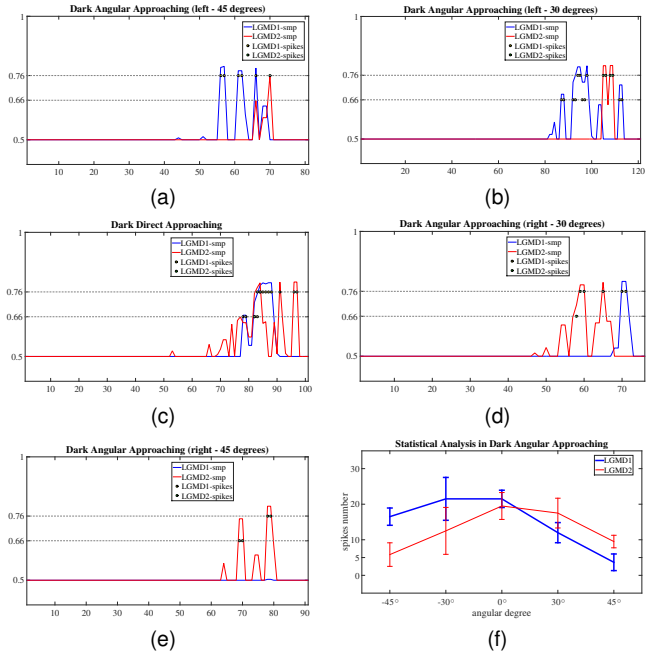

Fig. 7. The outputs of LGMD1 and LGMD2 neuron models challenged by the Colias robot approaching from two sides of different angles in the bright environment: (a), (b), (c), (d), (e) The neural potentials of LGMD1 and LGMD2 neurons are indicated by blue and red lines respectively. The elicited spikes are drawn at two spiking thresholds (horizontally gray-dashed lines). X and Y axes denote the time sequence in frames and SMP level respectively. (f) The statistical results with mean and variance information, each angle throughout 10 repeated tests.

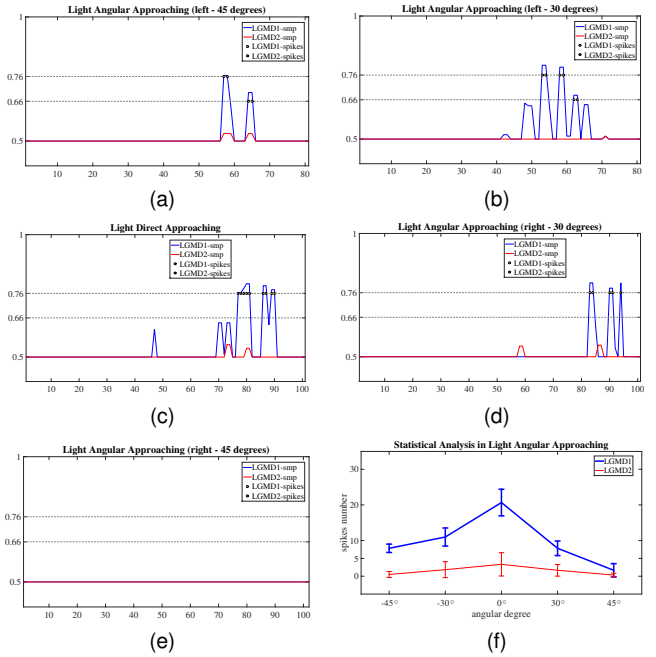

Fig. 8. The outputs of LGMD1 and LGMD2 neuron models and the statistical results challenged by angular approaches of lighter objects in the dark environment. Similarity for all the notations.

[5] J. Sztarker and F. C. Rind, "A look into the cockpit of the developing locust: looming detectors and predator avoidance," *Dev Neurobiol*, vol. 74, no. 11, pp. 1078–95, 2014.

[6] F. C. Rind, S. Wernitznig, P. Polt, A. Zankel, D. Gutl, J. Sztarker, and G. Leitinger, "Two identified looming detectors in the locust: ubiquitous lateral connections among their inputs contribute to selective responses to looming objects," *Scientific Reports*, 2016.

[7] S. Yue and F. C. Rind, "Collision detection in complex dynamic scenes using a lgmd based visual neural network with feature enhancement," *IEEE Trans. Neural Netw.*, vol. 17, no. 3, pp. 705–716, 2006.

[8] S. Bermudez i Badia, U. Bernardet, and P. F. Verschure, "Non-linear neuronal responses as an emergent property of afferent networks: a case study of the locust lobula giant movement detector," *PLoS Comput Biol*, vol. 6, no. 3, p. e1000701, 2010.

[9] M. Hongying, Y. Shigang, H. Andrew, A. Kofi, H. Mervyn, P. Nigel, H. Peter, and P. Cy, "A modified neural network model for lobula giant movement detector with additional depth movement feature," in *International Joint Conference on Nerual Networks 2009*. IEEE, 2009, Conference Proceedings, pp. 2078–2083.

[10] Q. Fu, C. Hu, and S. Yue, "Bio-inspired collision detector with enhanced selectivity for ground robotic vision system," in *British Machine Vision Conference 2016*, Conference Proceedings.

[11] Q. Fu and S. Yue, "Modelling lgmd2 visual neuron system," in *2015 IEEE 25th International Workshop on Machine Learning for Signal Processing (MLSP)*. IEEE, Conference Proceedings, pp. 1–6.

[12] S. Yue and F. C. Rind, "A collision detection system for a mobile robot inspired by locust visual system," in *Proc. IEEE Int. Conf. Robot. Autom.*, 2005, Conference Proceedings, pp. 3843–3848.

[13] S. Yue, R. D. Santer, Y. Yamawaki, and F. C. Rind, "Reactive direction control for a mobile robot: a locust-like control ofescape direction emerges when abilateral pair of model locust visual neurons are integrated," *Autonomous Robots*, vol. 28, no. 2, pp. 151–167, 2010.

[14] S. Yue and F. C. Rind, "Visually stimulated motor control for a robot with a pair of lgmd visual neural networks," *Int. J. Adv. Mechatron. Syst.*, vol. 4, no. 5, pp. 237–247, 2012.

[15] C. Hu, F. Arvin, C. Xiong, and S. Yue, "A bio-inspired embedded vision system for autonomous micro-robots: the lgmd case," *IEEE Transactions on Cognitive and Developmental Systems*, 2016.

[16] M. O'Shea and C. H. F. Rowell, "The neuronal basis of a sensory analyser, the acridid movement detector system. ii. response decrement, convergence, and the nature of the excitatory afferents to the fan-like dendrites of the lgmd," *J Exp Biol*, vol. 65, pp. 289–308, 1976.

[17] A. Borst and T. Euler, "Seeing things in motion: models, circuits, and mechanisms," *Neuron*, vol. 71, no. 6, pp. 974–94, 2011.

[18] Q. Fu and S. Yue, "Modeling direction selective visual neural network with on and off pathways for extracting motion cues from cluttered background," in *The 2017 International Joint Conference on Neural Networks*, 2017, Conference Proceedings.

[19] S. Peron and F. Gabbiani, "Spike frequency adaptation mediates looming stimulus selectivity in a collision-detecting neuron," *Nat Neurosci*, vol. 12, no. 3, pp. 318–26, 2009.

[20] S. D. Wiederman, P. A. Shoemaker, and D. C. O'Carroll, "Correlation between off and on channels underlies dark target selectivity in an insect visual system," *J Neurosci*, vol. 33, no. 32, pp. 13 225–13 232, 2013.

[21] S. Yue and F. C. Rind, "Near range path navigation using lgmd visual neural networks," in *Computer Science and Information Technology, ICCSIT*, 2009, Conference Proceedings, pp. 105–109.

[22] F. Arvin, J. Murray, C. Zhang, and S. Yue, "Colias: An autonomous micro robot for swarm robotic applications," *International Journal of Advanced Robotic Systems*, pp. 1–10, 2014.

[23] F. Arvin, A. E. Turgut, T. Krajník, and S. Yue, "Investigation of cue-based aggregation in static and dynamic environments with a mobile robot swarm." *Adaptive Behavior*, vol. 24, no. 2, pp. 102–118, 2016.

[24] F. Arvin, T. Krajnik, A. E. Turgut, and S. Yue, "Cos: Artificial pheromone system for robotic swarms research," in *2015 IEEE/RSJ International Conference on Intelligent Robots and Systems (IROS)*. IEEE, 2015, Conference Proceedings, pp. 407–412.

[25] P. Lightbody, M. Hanheide, and T. Krajnik, "A versatile high-performance visual fiducial marker detection system with scalable identity encoding," in *32nd ACM Symposium on Applied Computing*, 2017, Conference Proceedings, pp. 3–7.

[26] T. Krajník, M. Nitsche, I. Faigl, P. Vaněk, M. Saska, L. Přeučil, T. Duckett, and M. Marta, "A practical multirobot localization system," *Journal of Intelligent and Robotic Systems*, vol. 76, no. 3-4, pp. 539–562, 2014.